

RESEARCH ARTICLE

Open Access



Weighted minimum feedback vertex sets and implementation in human cancer genes detection

Ruiming Li¹, Chun-Yu Lin^{1,2,3}, Wei-Feng Guo⁴ and Tatsuya Akutsu^{1*} 

*Correspondence:

takutsu@kuicr.kyoto-u.ac.jp

¹ Bioinformatics Center,
Institute for Chemical
Research, Kyoto University,
Uji, Kyoto 611-0011, Japan
Full list of author information
is available at the end of the
article

Abstract

Background: Recently, many computational methods have been proposed to predict cancer genes. One typical kind of method is to find the differentially expressed genes between tumour and normal samples. However, there are also some genes, for example, 'dark' genes, that play important roles at the network level but are difficult to find by traditional differential gene expression analysis. In addition, network controllability methods, such as the minimum feedback vertex set (MFVS) method, have been used frequently in cancer gene prediction. However, the weights of vertices (or genes) are ignored in the traditional MFVS methods, leading to difficulty in finding the optimal solution because of the existence of many possible MFVSs.

Results: Here, we introduce a novel method, called weighted MFVS (WMFVS), which integrates the gene differential expression value with MFVS to select the maximum-weighted MFVS from all possible MFVSs in a protein interaction network. Our experimental results show that WMFVS achieves better performance than using traditional bio-data or network-data analyses alone.

Conclusion: This method balances the advantage of differential gene expression analyses and network analyses, improves the low accuracy of differential gene expression analyses and decreases the instability of pure network analyses. Furthermore, WMFVS can be easily applied to various kinds of networks, providing a useful framework for data analysis and prediction.

Keywords: Feedback vertex set, Differential gene expression, Cancer gene

Background

Cancer is a genetic disease, but not all genes are related to cancer. By almost universal consensus, cancer is now viewed as resulting from changes in some key regulatory genes [1]. At present, researchers have defined several kinds of cancer-related gene sets. One widely used kind of gene set is that of cancer driver genes, which are defined as genes whose mutations increase net cell growth under the specific microenvironmental conditions that exist in the cell in vivo. This kind of gene can be predicted by finding 'significantly mutated genes', whose mutation rates are significantly higher



© The Author(s) 2021. **Open Access** This article is licensed under a Creative Commons Attribution 4.0 International License, which permits use, sharing, adaptation, distribution and reproduction in any medium or format, as long as you give appropriate credit to the original author(s) and the source, provide a link to the Creative Commons licence, and indicate if changes were made. The images or other third party material in this article are included in the article's Creative Commons licence, unless indicated otherwise in a credit line to the material. If material is not included in the article's Creative Commons licence and your intended use is not permitted by statutory regulation or exceeds the permitted use, you will need to obtain permission directly from the copyright holder. To view a copy of this licence, visit <http://creativecommons.org/licenses/by/4.0/>. The Creative Commons Public Domain Dedication waiver (<http://creativecommons.org/publicdomain/zero/1.0/>) applies to the data made available in this article, unless otherwise stated in a credit line to the data.

than the presumed background somatic mutation rate [2–4]. However, since it is difficult to construct a reliable background mutation model [5], selecting gold-standard driver genes by frequency-based methods is difficult. Another kind of cancer-related genes are so-called ‘cancer genes’, including oncogenes, which function as positive growth regulators, and tumour suppressor genes (TSGs), which function as negative growth regulators. These genes are directly related to the phenotypes of tumour and normal genes and can be predicted by differential gene expression analyses. However, some ‘dark’ genes play important roles at the network level but are generally ignored by traditional differential gene expression analyses [6, 7].

By using graph theory algorithms, we can find critical vertices to control a network. For example, [8] developed a feedback-based framework that provides realizable node overrides that steer a system towards one of its natural long-term dynamic behaviours; [9] provided a rational criterion for selecting key molecules to control a system with a feedback vertex set (FVS); [10] proposed a network control strategy to find driver mutations that drive a regulation network from the normal state to a disease state; and [11] considered applying minimum feedback vertex sets (MFVS) to real biologically directed complex networks and found essential proteins in both *Drosophila melanogaster* and *Homo sapiens* organisms.

Given a directed network, a feedback vertex set (FVS) is a set of vertices whose removal leaves the remaining network acyclic. The minimum feedback vertex set (MFVS) is a kind of FVS that has the minimum size among all possible FVSs. The MFVS problem has been proven to be NP-complete [12]. There already exist many algorithms for solving the MFVS problem, including approximation algorithms [13], randomized algorithms [14], parameterized algorithms [15] and exact algorithms [16, 17].

Generally, a network can have multiple MFVSs. Traditional MFVS algorithms ignore the differences among possible MFVSs, and the output is usually random. This randomness leads to the instability of network analysis methods in practice. To find the best output from multiple MFVSs, in this paper, we consider a variation of the MFVS problem, i.e., each vertex is assigned a weight, and the output is the maximum total weighted MFVS. The assigned weight should reflect the significance of the corresponding vertex, which may involve some biological data from other studies (for example, in our experiments, we utilize the differential expression value to compute the weights). We define this problem as a weighted MFVS (WMFVS) problem.

To solve the WMFVS problem, we modified an exact algorithm from [17], which first compresses the original graph [18, 19] to reduce the number of vertices and arcs and then utilizes an integer linear programming (ILP) method for the compressed graph. Our WMFVS method can be roughly separated into three parts, i.e., graph compression, MFVS size determination and output optimization. The first two parts use the same idea as [17], and the third part uses the modified ILP method to select the maximum weighted MFVS.

Furthermore, we consider a variation of the WMFVS method that pays more attention to the total weight of an FVS than to its size; i.e., it finds the maximum-weighted FVS. We call this method WFVS. In the next sections, we can see that WMFVS has a higher precision than WFVS, while WFVS has an advantage in recall.

Results

Data sets

In this study, we used the directed human protein interaction network [20] for the analyses; it contains 6338 genes (vertices) and 34814 directed interactions (arcs). To evaluate the relative prediction accuracies for cancer genes between our methods and existing methods, we collected cancer-related gene sets from five public databases: ONGene [21], TSGene [22], CGC [23], NCG [24] and MSigDB C6 [25]. Since not all genes from the data sets are contained in the directed human protein interaction network, we filtered the common genes in both a certain data set and the network. The sizes of these data sets are shown in Table 1.

In the rest of this paper, when we calculate the recall of various methods, we consider only the size of the common gene sets.

Weight definition

To define the weights of genes, we first downloaded the RNA-seq data from TCGA [26], which contains gene expression data from 1102 breast tumour samples and 113 normal samples. Next, the counts of level 3 RNASeqV2 data were processed and transformed before being used for further analysis [27]. Specifically, we used the fold change (FC) value (with the binary logarithm and absolute value) between tumour and normal samples as the weight of each vertex (gene). For a specific gene v , its weight is calculated by the following formula:

$$v.w = \left| \frac{\sum_{i=1}^n \log_2 T_i}{n} - \frac{\sum_{j=1}^m \log_2 N_j}{m} \right| \quad (1)$$

where T_i is the expression value of tumour sample i , N_j is the expression value of a normal sample j , and n and m are the numbers of tumour and normal samples, respectively. Intuitively, a high FC value corresponds to a high possibility of a cancer gene. Thus, it is reasonable to use the FC values as the weights of genes.

For the genes that appear in the network but have no expression values in the TCGA data (only 143 genes, 2.3% of the network size; these are called weight-loss genes), we gave them default weights of 0 rather than ignoring them; thus, if such a gene is essential at the topological level, it has the potential to be selected as a cancer gene, which may counteract the disadvantage of the traditional differential expression-based methods in dark gene-revealing and missing-data situations. Finally, all 6338 genes in the graph were weighted. The topological structure of the graph remained the same as in the original protein interaction network.

Table 1 Size of each data set and the number of genes contained in the network (common genes)

	ONGene	TSGene	CGC	NCG	MSigDB
Number of genes	803	1217	723	2372	10,962
Common genes	490	641	525	1210	4184

Experiments and evaluation

The whole experiment process is shown in Fig. 1.

First, we analysed the directed human protein interaction network with traditional MFVSs and obtained a set of 463 vertices. Then, we used our WMFVS method on the same network (the weights were derived from the FC values). We also used the inverses of the weights as the penalty values and applied them to our WFVS method.

Because of the non-uniqueness of the MFVS method, it is not a general evaluation if we consider only one MFVS result. Therefore, we calculated a set of random MFVSs by applying the WMFVS method with randomly shuffled gene weights. First, we planned to compute 1000 random MFVSs for analysis. However, since the Gurobi optimizer (version 8.1.0) does not always output a real optimal solution (e.g., even when we restrict the size of the output to be exactly 463, which is the size of the MFVS, sometimes the sizes of the output are smaller than 463), we filtered the obviously incorrect results and verified all the other outputs as MFVSs. Finally, we obtained 875 approved random MFVSs (since some MFVSs may be lost in the *ignore_w* operation and the MFVSs are not distributed uniformly, not all possible MFVSs have the same possibility of random selection).

The WMFVS and WFVS result data can be found in the supplementary data. The random MFVS data are placed in https://github.com/lrming1993/WMFVS_codes.

To evaluate the results of these three methods, we first checked the graph-level results (see Table 2).

The run time of MFVS is due to the use of the traditional non-weighted MFVS method. The sum weight of MFVS uses the average value from 875 randomly weighted WMFVSs.

As we expected, the WMFVS method obtained a better total weight than the traditional MFVS. However, the result of WMFVS is not always better than that of MFVS. The total weight of the output of the traditional MFVS method is random (the output

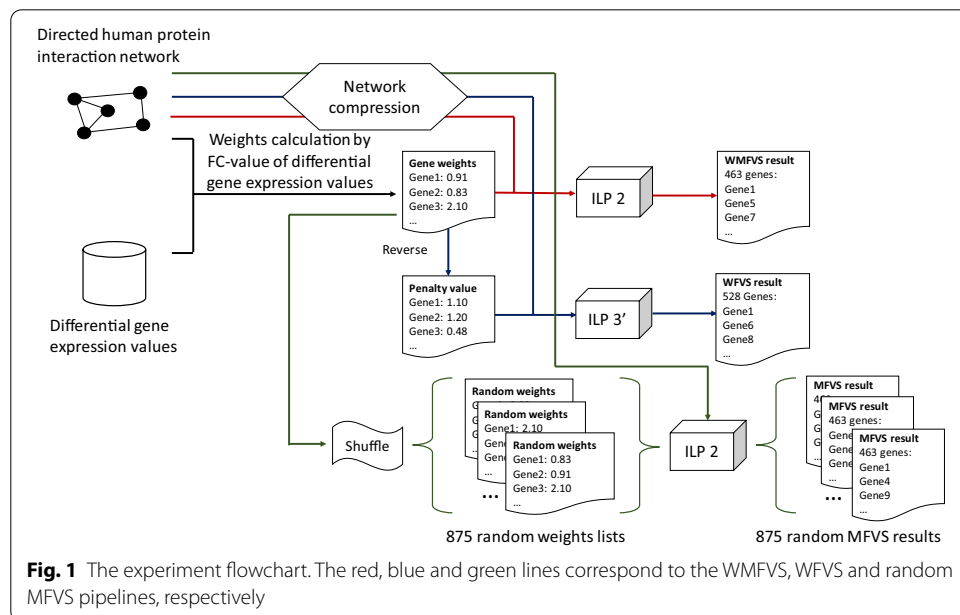
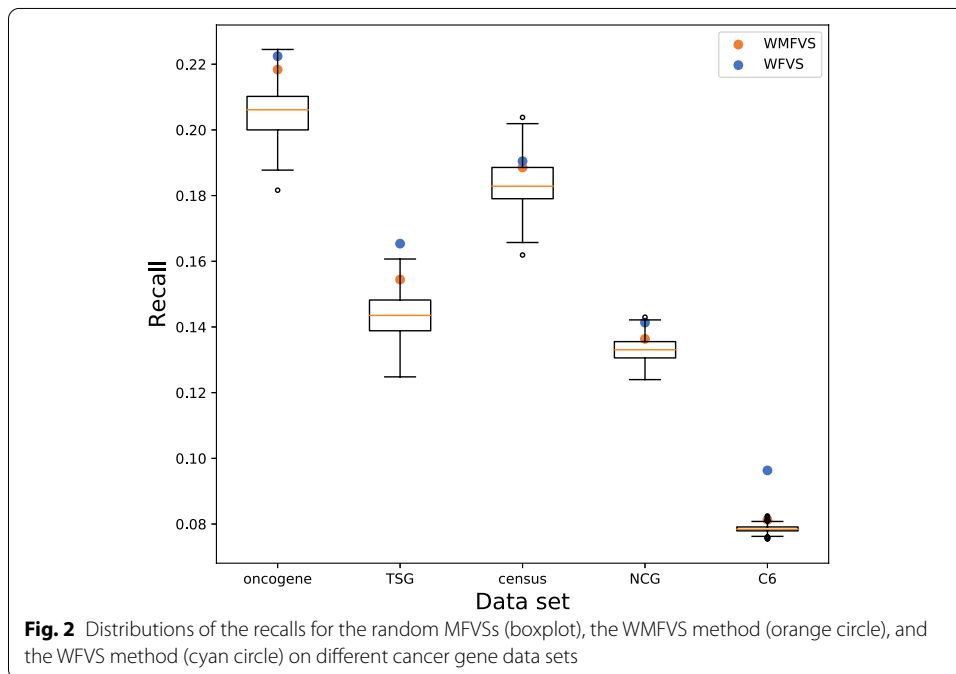


Table 2 The graph-level results of each method

	Output size	Run time (s)	Sum weight	Average weight of each vertex
MFVS	463	4.0	319.5	0.69
WMFVS	463	35.9	379.3	0.82
WFVS	528	23.6	496.4	0.94



is related to the graph structure but has no relevance to the vertex weights), so it is possible for MFVS to output a highly weighted vertex set, even higher than the weight of the calculated WMFVS (Gurobi may not always give a real optimal result because of its numerical instability). However, our WMFVS method clearly has better stability.

The WFVS method returned an FVS with 528 vertices, which is approximately 14% larger than the size of the MFVS. The selected WFVS has a better average weight than both the MFVS and WMFVS. This result is consistent with our purpose for WFVSs, which focuses on the total weight rather than the size of the FVS.

Then, we used the five prepared cancer-related gene data sets to evaluate the results of these three methods. We verified the recall of the three FVS methods in the five data sets. The results are shown in Table 3 and Fig. 2.

We can see that WMFVS and WFVS have better recall than traditional MFVS in all five sets, which is a benefit of the well-defined gene weights (especially for WFVS). Furthermore, we calculated the p-values of WMFVS and WFVS for 875 random MFVSs (Table 4).

For a certain data set, denote the recall of WMFVS by R_{WMFVS} . The recalls of all random MFVSs compose a set R_{random} . Then the p-value of WMFVS is calculated by the following formula:

Table 3 The recall of each method in different gene sets

	ONGene	TSGene	CGC	NCG	MSigDB
MFVS (average)	20.6%	14.4%	13.3%	13.2%	7.9%
WMFVS	21.8%	15.4%	18.8%	13.6%	8.1%
WFVS	22.2%	16.5%	19.0%	14.1%	9.6%

Table 4 The p-values of WMFVS and WFVS for random MFVSs

	ONGene	TSGene	CGC	NCG	MSigDB
WMFVS	0.0491	0.0434	0.2537	0.2011	0.0069
WFVS	0.0069	0.0	0.1771	0.0091	0.0

$$p_{WMFVS} = \frac{|\{R|R \geq R_{WMFVS}, R \in R_{random}\}|}{|R_{random}|} \quad (2)$$

The calculation of the p-value of WFVS is the same as above.

Next, as control methods, we considered several other kinds of methods of cancer gene prediction.

- (1) Randomly select 463 genes (select 100 times and take the average performance).
- (2) Select the 463 highest-weighted genes, which is a traditional differential expression-based method.
- (3) Select the set of genes that appear in at least 49.5% MFVSs (we used 49.5% since the number of genes was exactly 463).

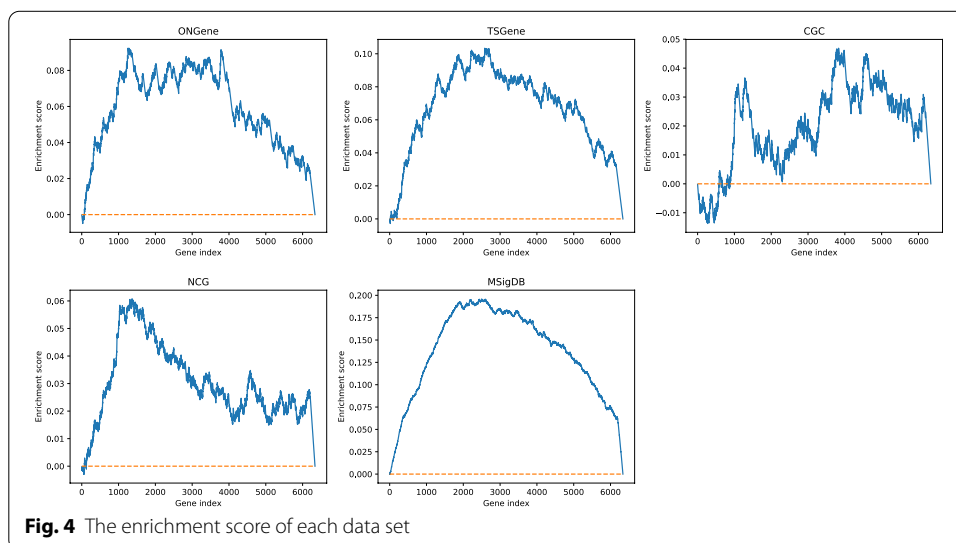
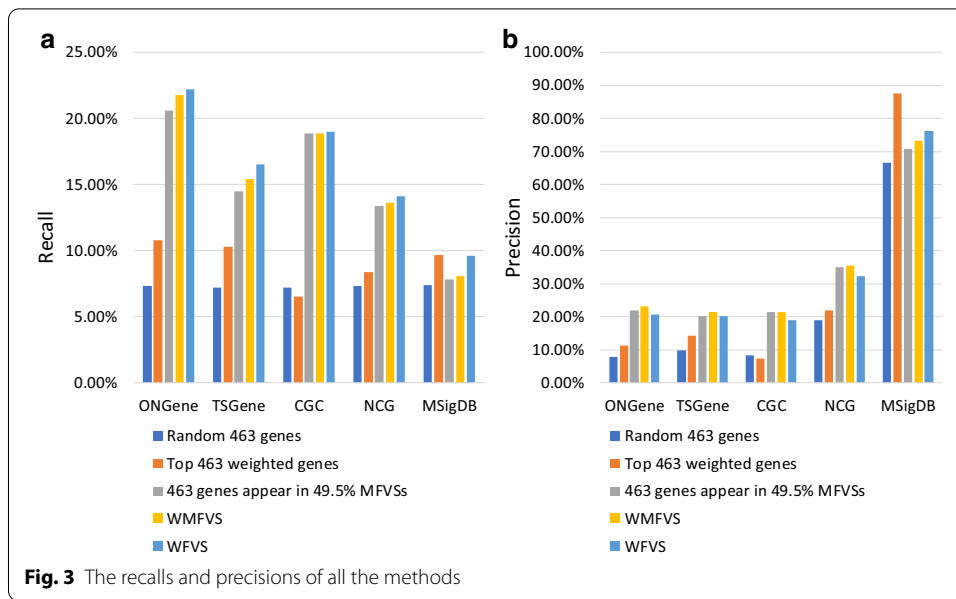
Method (2) uses only weights for classification (i.e., a pure differential expression analysis method), while method (3) uses only graph theoretic results (i.e., a pure network analysis method). Method (3) selects the most common genes that appear in the MFVS. Intuitively, these genes should have great significance in the graph topology. The recalls and precisions of all these methods are listed in Table 5. Additionally, see Fig. 3.

Discussion

Performance and enrichment score

In ONGene, TSGene and MSigDB, both WMFVS and WFVS have good p-values, but for CGC and NCG, the p-value is relatively high. One major reason is that there exists some correlation between the classification metric of the data set and the defined gene weight. To analyse this correlation, we utilized the enrichment score (ES) from GSEA [25], which reflects the degree to which a set S is overrepresented at the extremes (top or bottom) of an entire ranked list.

First, we sorted all the genes from the network by weight from high to low. Then, for a certain cancer gene set S , we traversed the sorted gene list, increasing a running-sum statistic when we encountered a gene in S and decreasing it when we encountered



a gene not in S . We modified the increment and decrement value to ensure that the running sum was 0 at the end of the gene list. The enrichment scores of the five data sets are shown in Fig. 4.

It is easy to see that the ONGene, TSGene and MSigDB data sets are significantly enriched at the tops of the lists. Although NCG seems enriched at the top, its ES is relatively low; the ES of CGC is even worse than that of NCG. The best enriched data set is MSigDB. Since this data set was constructed directly from microarray gene expression data from cancer gene perturbations, it is closely related to differential expression values. The ES value explains the different performances of WMFVS and WFVS in different data sets.

Table 5 The recalls (and precisions) of all the methods

	463 random genes	Top 463 weighted genes	Genes appearing in 49.5% MFVSs	WMFVS (size: 463)	WFVS (size: 528)
ONGene	7.3% (7.8%)	10.8% (11.4%)	20.6% (21.8%)	21.8% (23.1%)	22.2% (20.6%)
TSGene	7.2% (9.9%)	10.3% (14.3%)	14.5% (20.1%)	15.4% (21.4%)	16.5% (20.1%)
CGC	7.2% (8.2%)	6.5% (7.3%)	18.9% (21.4%)	18.9% (21.4%)	19.0% (18.9%)
NCG	7.3% (19.0%)	8.4% (22.0%)	13.4% (35.0%)	13.6% (35.6%)	14.1% (32.4%)
MSigDB	7.4% (66.5%)	9.7% (87.5%)	7.8% (70.8%)	8.1% (73.4%)	9.6% (76.3%)

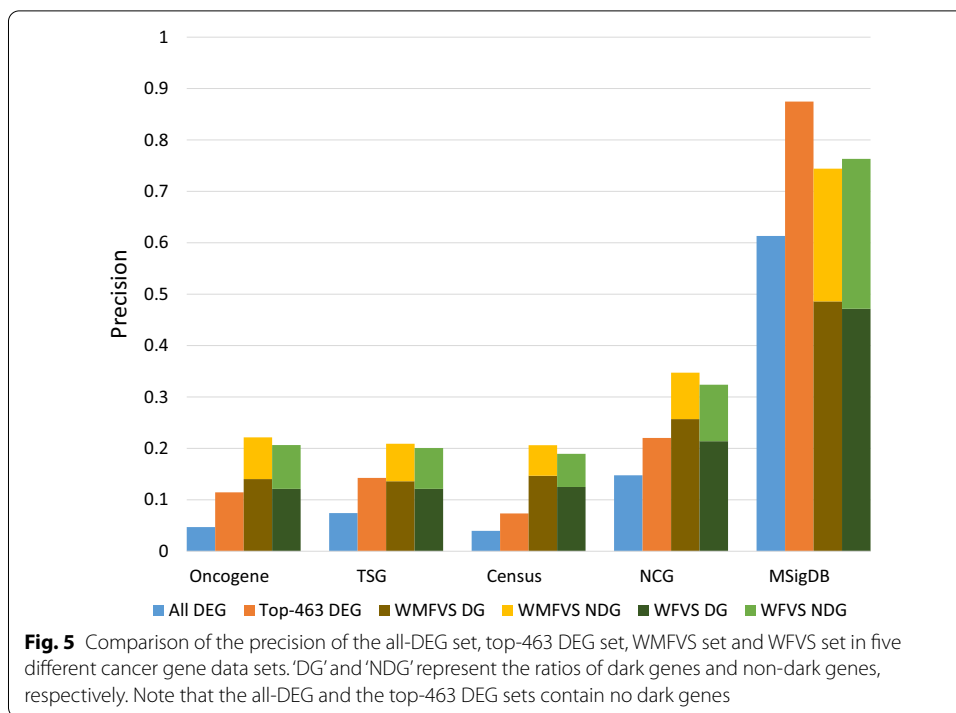
Table 5 and Fig. 3 show that, except in MSigDB, WMFVS has the best precision and WFVS has the best recall. In MSigDB, cancer genes are closely related to the differential expression values of genes in breast cancer, leading to a precision of 87.5% for the simple weight-based method (i.e., method (2)). In this case, integration of the network structure may decrease the precision. However, in most cases, it is hard to find such a closely related metric for classification. We can observe that in other data sets, method (2) performs worse than the other methods. The results support the effectiveness of our WMFVS and WFVS methods.

Dark genes

As mentioned previously, traditional differential expression-based methods are not able to find graph-level important genes that have low differential expression values, i.e., dark genes. In our research, we defined a dark gene as a gene that has a relatively low weight (i.e., a low differential expression value) but is recorded as a cancer gene in the cancer gene data base(s). Specifically, we first derived the differentially expressed genes (DEGs) by using the criteria of $|\log_2 FC| \geq 1$ and adjusted p-value ≤ 0.05 from the TCGA breast cancer RNA-seq data, where FC is the fold change value of a certain gene. Based on these criteria, we found 4245 DEGs (called the DEG set). Next, we curated the dark gene set from each cancer gene data set by excluding these DEGs.

In our experiments, we further selected the top 463 of the highest-weighted genes (i.e., the most differentially expressed genes; called the top-463 DEG set) to avoid an unbalanced gene number in comparison to the WMFVSs and WFVSs identified by the WMFVS and WFVS methods, respectively. For each of the cancer gene data sets, the precisions of the all-DEG set, top-463 DEG set, WMFVS and WFVS are shown in Fig. 5.

Figure 5 shows that our WMFVS and WFVS methods display better precision than the traditional DEG-based method (i.e., the all-DEG set and the top-463 DEG set) in four of five cancer gene data sets. Moreover, approximately 60–70% of the genes are dark genes, which were detected by using our WMFVS and WFVS methods but ignored by the traditional DEG method. Even for the MSigDB C6 data set, which was generated directly from microarray data or from internal unpublished profiling experiments involving the perturbation of known cancer genes, the WMFVS and WFVS methods also have a good ability to detect dark genes. In summary, our WMFVS and WFVS methods have an advantage in identifying dark genes that are hard to find by using traditional DEG methods.



Missing-data cases

In this study, to retain the topological structure of the network, the weight-loss genes are assigned default weights of 0 rather than being removed. By further analysis, we found 3 weight-loss genes (i.e., CDC2, ZBTB8 and TADA3L) included in the WMFVS result, 7 weight-loss genes (i.e., CDC2, ZBTB8, RhoGDI, TADA3L, RNF12, NP and MAP3K7IP1) contained in at least one of the 875 random MFVS results, and no weight-loss genes in the WFVS result. In particular, CDC2 and ZBTB8 were included in all the random MFVS results as well as in the WMFVS result. The CDC2 gene is related to the highly conserved protein CDK1, which functions as a serine/threonine kinase and is a key player in cell cycle regulation [28]. The CDC2 gene is also considered a cancer-related gene whose overexpression may play an important role in human breast carcinogenesis [29]. While little is known about the ZBTB8 gene, the same ZBTB family protein, ZBTB7A, has been implicated in high expression in cancer tissue and the breast cancer cell lines MDA-MB-231 and MCF-7 [30], suggesting that ZBTB8 may act as a transcriptional repressor or be involved in tumorigenesis. The uncovering of CDC2 and ZBTB8 genes illustrates that the WMFVS method may address the disadvantage of traditional DEG methods in missing-data cases.

Conclusion

We present several new methods for cancer gene prediction. Our WMFVS method uses differential gene expression to select MFVSs, improving the stability of the general MFVS algorithm and obtaining a much better result than the differential gene expression-based method when the weights of the genes are well defined. Our WFVS method is a variant of WMFVS, which aims at finding an FVS in the network that

contains the maximum total weight. This method obtains better recall than WMFVS by sacrificing precision. Thus, generally, if the researcher wants to reveal as many potential cancer genes as possible, WFVS is better; if the researcher prefers better precision, then WMFVS is better. Furthermore, since WFVS ignores the restriction of the output size, it focuses more on the vertex weight than WMFVS. Therefore, if the researcher has good confidence in the weight definition, i.e., the weights are closely related to the classification, WFVS will have a better result than WMFVS. We can see this from the data analyses on the MsigDB data set, which has the highest enrichment score on our defined weights. However, in many cases, since we are not sure whether the defined weights are closely related to the classification, using WMFVS will maintain better precision for the prediction.

WMFVS and WFVS take advantage of both bio-data and the network structure. They can be useful in novel cancer gene prediction and evaluation, and the same idea may also be applied to other bioinformatics problems. The main challenge of our methods is the definition of the weights. WMFVS and WFVS can perform very well when the weights are well defined but may display limited performance when the weights are not directly related to the category. Another issue concerns graph compression. In our experiments, the traditional MFVS method analysed the compressed graph (with the *ignore* operation; see details in the next section), which contained 660 vertices and 5604 arcs, and it was efficient and took only approximately 4 seconds to obtain the result. The input graph of WMFVS and WFVS was compressed using the limited *ignore_w* operation (see details in the next section), which contained 2348 vertices and 17283 arcs. Because of the different input scales, WMFVS and WFVS were not as efficient as the simple MFVS method, although the time costs were still acceptable. The development of new algorithms for weighted graph compression is left as future work.

Methods

Graph compression

In biological networks, a network usually contains tens of thousands of vertices and hundreds of thousands of arcs. In many cases, processing a large network is not practical because of the NP-hardness of the MFVS problem [12]. Generally, we can compress the original graph to a simpler graph that maintains (or can restore) the size of the MFVS of the original graph.

In the following sections, we define $v.suc$ and $v.pre$ as the sets of successors and predecessors of vertex v , respectively. Let v_i be a vertex in a network S . Consider the following three cases [18]:

- C1. $v_i \in v_i.suc$, i.e., v_i has a self-loop; then, v_i should be in all FVSs, otherwise the self-loop cannot be removed.
- C2. $v_i.suc = \emptyset$ (or $v_i.pre = \emptyset$); then, v_i is not in any MFVS, since it is not in any cycle.
- C3. $|v_i.suc| = 1$ (or $|v_i.pre| = 1$); let v_j be the only successor (or predecessor, respectively) of v_i ; then, any cycle containing v_i also contains v_j .

For C1, we use a temporary list ΔM to record v_i ; we add v_i to ΔM and remove v_i and all its incoming and outgoing arcs from the graph. We use $remove(v_i)$ to denote this removing process.

For C2, since v_i is not in any MFVS, we can safely use $remove(v_i)$ without any change to the possible MFVSs.

For C3, assume v_i is in some cycle c . If we attempt to break c by removing v_i , then it is equally good (sometimes better) to remove v_j rather than v_i . Here, we connect all predecessors of v_i to all its successors and then use $remove(v_i)$. We denote this connecting and removing operation by $ignore(v_i, S)$, where S is the current graph to which v_i belongs. The procedure is as follows:

Procedure 1 $ignore(v, S)$

```

1: for  $v_i \in v.pre$  do
2:   for  $v_j \in v.suc$  do
3:     if  $(v_i, v_j) \notin S.E$  then
4:        $S.E := S.E \cup (v_i, v_j)$ 
5:     end if
6:   end for
7: end for
8:  $remove(v)$ 

```

In the above procedure, v is a vertex in graph S , and $S.E$ is the arc set of graph S . Then we have the following procedure to compress a graph S :

Procedure 2 $compress_vertex(S)$

```

1:  $\Delta M := \emptyset$ 
2: for  $v_i \in S.V$  do
3:   if  $v_i \in v_i.suc$  then
4:      $\Delta M := \Delta M \cup v_i$ ;
5:      $remove(v_i)$ 
6:   else if  $|v_i.suc| == 0$  or  $|v_i.pre| == 0$  then
7:      $remove(v_i)$ 
8:   else if  $|v_i.suc| == 1$  or  $|v_i.pre| == 1$  then
9:      $ignore(v_i, S)$ 
10:   end if
11: end for

```

We repeat this procedure until S cannot be modified.

Furthermore, we use the strongly connected components (scc's) [17, 19] to reduce the arcs. Since an arc between two scc's is not in any cycle, the deletion of these arcs will not change any MFVSs. We use $compress_scc(S)$ to denote the operation that removes all arcs between two different scc's in S . The whole graph compressing procedure is as follows:

Procedure 3 *compress_graph*(S)

```

1:  $\Delta M := \emptyset$ 
2: do
3:   compress_scc( $S$ )
4:    $\Delta M := \Delta M \cup \text{compress\_vertex}(S)$ 
5: while  $S$  is modified and  $S.V \neq \emptyset$ 
6: return  $\Delta M$ 

```

The returned ΔM contains the vertices that are always in any MFVS, and the union of ΔM and any MFVS of the compressed graph will be an MFVS of the original graph.

Note that not all MFVSs of the original graph can be obtained from the above method. Some MFVSs are lost in the *ignore* operation, while in a weighted MFVS problem, the lost MFVSs may have the maximum weight. For the weighted case, we modify the *ignore* operation to consider the weights of vertices (only for positive-weighted cases). The following method ensures that the maximum-weight MFVS (the WMFVS) will not be lost:

Procedure 4 *ignore_w*(v, S)

```

1: if  $|v.suc| == 1$  then
2:   let  $v'$  be the only successor of  $v$ 
3:   if  $v.w < v'.w$  then
4:     ignore( $v, S$ )
5:   end if
6: else if  $|v.pre| == 1$  then
7:   let  $v'$  be the only predecessor of  $v$ 
8:   if  $v.w < v'.w$  then
9:     ignore( $v, S$ )
10:  end if
11: end if

```

where $v.w$ denotes the weight of vertex v .

Theorem 1 *When the weights of the vertices are positive, the vertices ignored in the *ignore_w* procedure are not in any WMFVS.*

Proof

Assume $v.pre = \{v'\}$, $v.w < v'.w$, and v belongs to a WMFVS M . Then, $v' \notin M$, otherwise $M' := M - \{v\}$ is still an FVS, which has fewer vertices than an MFVS.

Now consider $M'' := (M - \{v\}) \cup \{v'\}$. It is obvious that M'' is an MFVS. Since $v'.w > v.w$, we have $\sum_{v_i \in M} v_i.w < \sum_{v_j \in M''} v_j.w$. Thus, M cannot be a WMFVS, i.e., if v has only one predecessor and the weight of v is less than that of the predecessor, then v does not belong to any WMFVS.

The proof is similar when v has only one successor and the weight of v is less than that of the successor. \square

ILP formulation for MFVS and WMFVS

After the compressing procedure, if the compressed graph is not empty, we can use an ILP method [17] to solve the remaining MFVS problem. For each remaining vertex v_i , we add two parameters x_i (Boolean) and k_i (integer), where x_i denotes whether v_i is included in the output MFVS result and k_i is a temporary parameter used in the ILP. The ILP formulation is as follows:

ILP1:

$$\begin{aligned}
 &\text{Minimize} && \sum x_i \\
 &\text{Subjectto} && k_i - k_j + nx_i \geq 1 \forall (v_i, v_j) \in E \\
 &&& \text{where } 0 \leq k_i \leq n - 1 \text{ and } x_i \text{ is Boolean}
 \end{aligned}$$

where E is the arc set of the remaining graph.

These constraints ensure that the selected vertices compose an FVS of S , while the objective function means that the selected FVS has a minimum size, i.e., it is an MFVS.

Now we consider the weighted case of the MFVS problem. Given a graph S , where each vertex $v_i \in S.V$ has a weight $v_i.w$ (in what follows, we use w_i to denote $v_i.w$ if there is no ambiguity), the WMFVS problem is to find an MFVS of S that has the maximum total weight. Assuming we already know the size s of the MFVS (by ILP1 or some estimation method such as that of [31] or [32]), the following formulation optimizes the selected MFVS as a WMFVS:

ILP2:

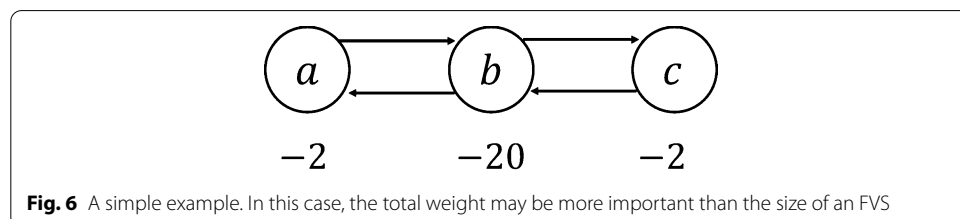
$$\begin{aligned}
 &\text{Maximize} && \sum w_i x_i \\
 &\text{Subjectto} && \sum x_i = s \\
 &&& k_i - k_j + nx_i \geq 1 \forall (v_i, v_j) \in E \\
 &&& \text{where } 0 \leq k_i \leq n - 1 \text{ and } x_i \text{ is Boolean}
 \end{aligned}$$

The constraint $\sum x_i = s$ ensures that the selected FVS is an MFVS, while the objective function selects the maximum-weight MFVS among all possible MFVSs.

Maximum-weight FVS

In the WMFVS problem, we first restrict the size of the FVS to be minimal and then select the maximum-weight MFVS as the objective. However, sometimes the weight may be more important than the size of an FVS. As an example, in Fig. 6, the WMFVS is $\{b\}$, which has a total weight of -20 . If we do not restrict the minimum size of the set, the FVS $\{a, c\}$, which has weight -4 , seems better.

Here we define a variant of the WMFVS problem, which ignores the exact size of the output vertex set, as follows: Given a graph S , where each vertex $v_i \in S.V$ has a weight $v_i.w$ (or w_i), the weighted FVS (WFVS) problem is to find an FVS of S that



has the maximum total weight. We can simply use a similar ILP as ILP2 to solve the WFVS problem.

ILP3:

$$\begin{array}{ll} \text{Maximize} & \sum w_i x_i \\ \text{Subjectto} & k_i - k_j + nx_i \geq 1 \forall (v_i, v_j) \in E \\ & \text{where } 0 \leq k_i \leq n - 1 \text{ and } x_i \text{ is Boolean} \end{array}$$

However, simply removing the constraint $\sum x_i = s$ may lead to a trivial solution when the weights of the vertices are positive, since the set of all vertices will always be a WFVS. Here we consider two methods to avoid the trivial solution:

1. Modify all weights to be negative. Assume the maximum weight of the vertices is w_m ; then, for each weight w_i , modify it to $w_i := w_i - w_m - \epsilon$. Here, ϵ is a small positive constant to ensure that all weights are negative. The ILP is the same as ILP3.
2. Reverse the weights to penalty values. We can simply do this by taking the inverse of each w_i , i.e.,

$$p_i = \begin{cases} \frac{1}{w_i} & \text{if } w_i \neq 0 \\ \infty & \text{if } w_i = 0 \end{cases}$$

Then, modify the ILP3 formula as follows: **ILP3'**:

$$\begin{array}{ll} \text{Minimize} & \sum p_i x_i \\ \text{Subjectto} & k_i - k_j + nx_i \geq 1 \forall (v_i, v_j) \in E \\ & \text{where } 0 \leq k_i \leq n - 1 \text{ and } x_i \text{ is Boolean} \end{array}$$

In our research, we examined both ways of calculating the weights in the WFVS method. We found that the first modification is more unstable when running the ILP process, i.e., more obviously wrong ILP results appeared. Thus, we chose to use the second method to compute the weights in the WFVS method; i.e., we reversed the weights to be penalty values, which are always positive values.

In the second method, we need to avoid the 'division by zero' error. To this end, we used the simple heuristic formula below.

Let l be a large number (in our program, we used 65536); then, the penalty is calculated by:

$$p_i = \begin{cases} \frac{1}{w_i} & \text{if } w_i \geq \frac{1}{l} \\ l & \text{if } w_i < \frac{1}{l} \end{cases}$$

Experimental environment

We implemented all the methods in Python 3.7.0 with an Intel(R) Core(TM) i7-7700 CPU and 32.0 GB RAM. The *compress_scc* procedure uses Gabow's algorithm [33]. The ILP processing is based on Gurobi 8.1.0 [34].

Abbreviations

MFVS: Minimum feedback vertex set; WMFVS: Weighted minimum feedback vertex set; WFVS: Maximum weighted feedback vertex set; ILP: Integer linear programming; FC: Fold change; ES: Enrichment score; scc: Strongly connected component; DEG: Differentially expressed gene.

Supplementary Information

The online version supplementary material available at <https://doi.org/10.1186/s12859-021-04062-2>.

Additional file 1. The data of the edges of the compressed network; the *ignore* operation was used. This file was used for the traditional MFVS computation.

Additional file 2. The data of edges of the compressed network; neither *ignore* nor *ignore_w* was used. This file was used for WFVS computation.

Additional file 3. The data of the edges of the compressed network; the *ignore_w* procedure was used. This file was used for WMFVS computation.

Additional file 4. The weights of all genes in the network.

Additional file 5. The ΔM computed from procedure 3, where the *ignore* operation was used. This file is necessary when using Additional file 1 to compute the MFVS.

Additional file 6. The ΔM computed from procedure 3, where the *ignore_w* operation was used. This file is necessary when using Additional file 3 to compute the WMFVS.

Additional file 7. The result of the traditional MFVS method.

Additional file 8. The result of the WMFVS method.

Additional file 9. The result of the WFVS method.

Acknowledgements

Not applicable.

Author's contributions

TA and CL conceived and designed the study. TA and RL designed the algorithms. RL, CL and WG prepared the experimental data. RL performed all the implementations and result analysis. RL produced the first draft. All authors took part in finalizing the manuscript and have approved the submitted draft.

Funding

This work was partially supported by (1) the International Collaborative Research Program of Institute for Chemical Research, Kyoto University, Japan; (2) the Young Scholar Fellowship Program by the Ministry of Science and Technology (MOST) in Taiwan, under Grant MOST 109-2636-B-009-007; (3) the Center for Intelligent Drug Systems and Smart Bio-devices (IDS²B) of the Higher Education Sprout Project (HESP) by the Ministry of Education (MOE), Taiwan; (4) the 'Smart Platform of Dynamic Systems Biology for Therapeutic Development' from The Featured Areas Research Center Program within the framework of the HESP by the MOE, Taiwan; (5) the National Natural Science Foundation of China (No. 62002329); (6) the Key scientific and technological projects of Henan Province (212102310083); (7) the Henan postdoctoral research start project in 2020; and (8) the Research start-up funds for top doctors in Zhengzhou University (32211739). The funding bodies did not play any role in the design of the study and collection, analysis, and interpretation of data and in writing the manuscript.

Availability of data and materials

The source code is on GitHub (https://github.com/lrming1993/WMFVS_codes). The random MFVS results can also be found at this URL. All data generated during this study are included in this published article and its supplementary information files.

Declarations

Ethics approval and consent to participate

Not applicable.

Consent to publication

Not applicable.

Competing interests

TA is an Associate Editor of *BMC Bioinformatics*.

Author details

¹ Bioinformatics Center, Institute for Chemical Research, Kyoto University, Uji, Kyoto 611-0011, Japan. ² Institute of Bioinformatics and Systems Biology, National Yang Ming Chiao Tung University, 300 Hsinchu, Taiwan. ³ Center for Intelligent Drug Systems and Smart Bio-devices, National Yang Ming Chiao Tung University, 300 Hsinchu, Taiwan. ⁴ School of Electrical Engineering, Zhengzhou University, 450001 Zhengzhou, China.

Received: 22 June 2020 Accepted: 3 March 2021

Published online: 22 March 2021

References

- Vogt PK. Cancer genes. *West J Med.* 1993;158(3):273–8.
- Luo P, Ding Y, Lei X, Wu FX. deepDriver: predicting cancer driver genes based on somatic mutations using deep convolutional neural networks. *Front Genet.* 2019;10:13.
- Tokheim CJ, Papadopoulos N, Kinzler KW, Vogelstein B, Karchin R. Evaluating the evaluation of cancer driver genes. *Proc Natl Acad Sci.* 2016;113(50):14330–5.
- Parmigiani G, Boca S, Lin J, Kinzler KW, Velculescu V, Vogelstein B. Design and analysis issues in genome-wide somatic mutation studies of cancer. *Genomics.* 2009;93(1):17.
- Cheng F, Zhao J, Zhao Z. Advances in computational approaches for prioritizing driver mutations and significantly mutated genes in cancer genomes. *Briefings Bioinf.* 2016;17(4):642–56.
- Dai H, Li L, Zeng T, Chen L. Cell-specific network constructed by single-cell RNA sequencing data. *Nucleic Acids Res.* 2019;47(11):62–62.
- Ebbert MT, Jensen TD, Jansen-West K, Sens JP, Reddy JS, Ridge PG, Kauwe JS, Belzil V, Pregel L, Carrasquillo MM, et al. Systematic analysis of dark and camouflaged genes reveals disease-relevant genes hiding in plain sight. *Genome Biol.* 2019;20(1):97.
- Zañudo JGT, Yang G, Albert R. Structure-based control of complex networks with nonlinear dynamics. *Proc Natl Acad Sci.* 2017;114(28):7234–9.
- Mochizuki A, Fiedler B, Kurosawa G, Saito D. Dynamics and control at feedback vertex sets. II: a faithful monitor to determine the diversity of molecular activities in regulatory networks. *J Theor Biol.* 2013;335:130–46.
- Guo WF, Zhang SW, Liu LL, Liu F, Shi QQ, Zhang L, Tang Y, Zeng T, Chen L. Discovering personalized driver mutation profiles of single samples in cancer by network control strategy. *Bioinformatics.* 2018;34(11):1893–903.
- Bao Y, Hayashida M, Liu P, Ishitsuka M, Nacher JC, Akutsu T. Analysis of critical and redundant vertices in controlling directed complex networks using feedback vertex sets. *J Comput Biol.* 2018;25(10):1071–90.
- Garey MR, Johnson DS. *Computers and intractability.* San Francisco: Freeman; 1979.
- Guruswami V, Lee E. Inapproximability of feedback vertex set for bounded length cycles. In: *Electronic colloquium on computational complexity (ECCC)*, vol. 21; 2014. p. 2
- Becker A, Bar-Yehuda R, Geiger D. Randomized algorithms for the loop cutset problem. *J Artif Intell Res.* 2000;12:219–34.
- Cao Y, Chen J, Liu Y. On feedback vertex set: new measure and new structures. *Algorithmica.* 2015;73(1):63–86.
- Fomin FV, Villanger Y. Finding induced subgraphs via minimal triangulations. 2009. arXiv preprint [arXiv:0909.5278](https://arxiv.org/abs/0909.5278)
- Chakradhar ST, Balakrishnan A, Agrawal VD. An exact algorithm for selecting partial scan flip-flops. *J Electron Test.* 1995;7(1–2):83–93.
- Lloyd EL, Soffa ML, Wang CC. On locating minimum feedback vertex sets. *J Comput Syst Sci.* 1988;37(3):292–311.
- Smith G, Walford R. The identification of a minimal feedback vertex set of a directed graph. *IEEE Trans Circuits Syst.* 1975;22(1):9–15.
- Vinayagam A, Stelzl U, Foulle R, Plassmann S, Zenkner M, Timm J, Assmus HE, Andrade-Navarro MA, Wanker EE. A directed protein interaction network for investigating intracellular signal transduction. *Sci Signaling.* 2011;4(189):8–8.
- Liu Y, Sun J, Zhao M. ONGene: a literature-based database for human oncogenes. *J Genet Genomics.* 2017;44(2):119–21.
- Zhao M, Sun J, Zhao Z. TSGene: a web resource for tumor suppressor genes. *Nucleic Acids Res.* 2013;41(D1):970–6.
- Sondka Z, Bamford S, Cole CG, Ward SA, Dunham I, Forbes SA. The COSMIC Cancer Gene Census: describing genetic dysfunction across all human cancers. *Nat Rev Cancer.* 2018;18(11):696–705.
- Repana D, Nulsen J, Dressler L, Bortolomeazzi M, Venkata SK, Tourna A, Yakovleva A, Palmieri T, Ciccarelli FD. The Network of Cancer Genes (NCG): a comprehensive catalogue of known and candidate cancer genes from cancer sequencing screens. *Genome Biol.* 2019;20(1):1.
- Subramanian A, Tamayo P, Mootha VK, Mukherjee S, Ebert BL, Gillette MA, Paulovich A, Pomeroy SL, Golub TR, Lander ES, et al. Gene set enrichment analysis: a knowledge-based approach for interpreting genome-wide expression profiles. *Proc Natl Acad Sci.* 2005;102(43):15545–50.
- Weinstein JN, Collisson EA, Mills GB, Shaw KRM, Ozenberger BA, Ellrott K, Shmulevich I, Sander C, Stuart JM, Network CGAR, et al. The cancer genome atlas pan-cancer analysis project. *Nat Genet.* 2013;45(10):1113.
- Lin CY, Lee CH, Chuang YH, Lee JY, Chiu YY, Lee YHW, Jong YJ, Hwang JK, Huang SH, Chen LC, et al. Membrane protein-regulated networks across human cancers. *Nat Commun.* 2019;10(1):1–17.
- Morgan DO. *The Cell Cycle: Principles of Control.* London: New Science Press; 2007.
- Chae SW, Sohn JH, Kim D-H, Choi YJ, Park YL, Kim K, Cho YH, Pyo J-S, Kim JH. Overexpressions of Cyclin B1, cdc2, p16 and p53 in human breast cancer: the clinicopathologic correlations and prognostic implications. *Yonsei Med J.* 2011;52(3):445–53.
- Mao A, Chen M, Qin Q, Liang Z, Jiang W, Yang W, Wei C. ZBTB7A promotes migration, invasion and metastasis of human breast cancer cells through NF- κ B-induced epithelial-mesenchymal transition in vitro and in vivo. *J Biochem.* 2019;166(6):485–93.
- Jiang W, Liu T, Ren T, Xu K. Two hardness results on feedback vertex sets. In: *Frontiers in algorithmics and algorithmic aspects in information and management.* Berlin: Springer; 2011. pp. 233–243
- Madelaine FR, Stewart IA. Improved upper and lower bounds on the feedback vertex numbers of grids and butterflies. *Discrete Math.* 2008;308(18):4144–64.
- Gabow HN. Path-based depth-first search for strong and biconnected components. *Inf Process Lett.* 2000;74:107–14.

34. Gurobi Optimization L. Gurobi optimizer reference manual (2020). <http://www.gurobi.com>

Publisher's Note

Springer Nature remains neutral with regard to jurisdictional claims in published maps and institutional affiliations.

Ready to submit your research? Choose BMC and benefit from:

- fast, convenient online submission
- thorough peer review by experienced researchers in your field
- rapid publication on acceptance
- support for research data, including large and complex data types
- gold Open Access which fosters wider collaboration and increased citations
- maximum visibility for your research: over 100M website views per year

At BMC, research is always in progress.

Learn more biomedcentral.com/submissions

